International Journal of Bifurcation and Chaos, Vol. 21, No. 10 (2011) 2905–2917

DOI: 10.1142/S0218127411030222

TANGENS HYPERBOLICUS APPROXIMATIONS OF THE SPATIAL MODEL OF FRICTION COUPLED WITH ROLLING RESISTANCE

GRZEGORZ KUDRA and JAN AWREJCEWICZ
Department of Automation and Biomechanics (K–16),
Technical University of Lodz,
1/15 Stefanowskiego St., 90-924 Łódź, Poland

Received April 15, 2010; Revised September 20, 2010

In this paper, for the first time, the complete set of Tangens hyperbolicus approximations of model of dry friction coupled with rolling resistance for circular contact area between interacting bodies is proposed. The developed approximations are compared with corresponding Padé approximants of the first and second order well known from the literature and with the numerical solution of the exact integral model as well. It is shown that Tangens hyperbolicus approximants are closest to the exact solution. Then the approximated models are applied to the celtic stone dynamics, however with the significant simplifying assumption of circular contact between stone and the table, presenting differences between them again. Certain specific approximations and regularizations of the friction and rolling resistance models enabling and facilitating their application to the real problem are shown. The analysis of the response dependence on initial conditions is performed by the use of a special kind of diagram.

Keywords: Coulomb–Contensou friction model; friction modeling; rolling resistance; Tangens hyperbolicus approximation; Padé approximation; wobblestone; celt.

1. Introduction

In physics and technology there are many examples of systems which can be described as working in different modes with the transitions between corresponding modes very short in time when compared with the time duration of the modes. In mechanics, mainly the systems with impacts and dry friction belong to this class. Very often the transitions between modes are modeled as instantaneous and the system can be described by the use of the piecewise smooth differential equations (PWS). Then the PWS systems can be classified according to the degree of nonsmoothness in the following manner [Leine & Nijmeijer, 2004; Simpson, 2010]: (i) systems with a discontinuous Jacobian matrix but with continuous and nonsmooth vector field; (ii) systems with discontinuous vector field but with continuous and nonsmooth system state; (iii) systems with discontinuous system state (a combination of differential equations and maps, sometimes referred to as hybrid systems). The mechanical example of the system belonging to the first group is the system with stiffness being a nonsmooth continuous function of the position. Mechanical systems with dry friction are often modeled as systems possessing discontinuous damping characteristics (the second group) [Galvanetto, 2001]. The mechanical system can also possess a discontinuous stiffness characteristics. In particular, systems with impacts can be modeled as systems with discontinuous stiffness (the second group) if one assumes the model of compliant impacting bodies [Brogliato, 1999; Ivanov, 1996; Shaw & Holmes, 1983]. But usually the mechanical impacts are modeled assuming rigidity

of the impacting bodies. In this case the model belongs to the third group and impacts are often modeled by the use of Newtons' law based on the restitution coefficient [Brogliato, 1999; Awrejcewicz *et al.*, 2004; Awrejcewicz & Kudra, 2005a, 2005b]. Impacts and dry friction can appear simultaneously in mechanical systems as independent [Virgin & Begley, 1999] or coupled phenomena [Leine *et al.*, 2001].

Some approaches in modeling of mechanical systems with rigid limiters of motion can lead to PWS system of the third group with some state subspaces governed by the smooth differential equations supplemented by algebraic equations i.e. differential-algebraic equations (DAEs) [Awrejcewicz *et al.*, 2004; Awrejcewicz & Kudra, 2005a, 2005b]. It is related to the state of the system sliding along the obstacle.

The PWS systems of the second group (the first group also as the subclass) are called Fillipov's systems and the special theory for them exists [Fillipov, 1988] based on the convex analysis where the PWS differential equations are treated as equations with set-valued (multivalued) right-hand sides (differential inclusions) on the boundaries between subspaces where the functions are smooth. The convex analysis is also used to describe systems with impacts and friction [Moreau, 1988; Glocker, 1999, 2001; Pfeiffer & Glocker, 1996]. In this case, the PWS system of the third group (impulsive systems with Dirac pulse at impact instance) is treated as differential measure inclusion.

The problem of seeking the mode of the system in the next time instance (especially important when the system is on switching boundary) can be formulated by the use of algebraic inclusion leading to the nonlinear complementarity problem (NCP) in general or linear complementarity problem (LCP) for some special cases [Glocker, 1999; Pfeiffer, 2003; Pfeiffer & Glocker, 1996]. For the solution of algebraic inclusion in frictional contact problems the augmented Lagrangian method (ALM) can also be used [Leine & Nijmeijer, 2004].

The numerical methods for the simulation of the mechanical systems with frictional contacts can be divided into the following groups [Leine & Nijmeijer, 2004]: (a) regularization methods; (b) event driven integration methods; (c) time stepping methods. The regularization methods [Awrejcewicz *et al.*, 2008] based on the smoothing of the PWS or differential inclusions systems, results in smooth differential equations allowing for the use of classical integration methods. One of the serious disadvantages of this method is stiffness of the obtained problem. Another is that of possible loss of some original physical properties of the system. The event driven integration methods [Awrejcewicz & Kudra, 2005a; Glocker, 1999; Pfeiffer & Glocker, 1996] uses classical integration methods between switches (transition between modes) and LCP, NCP or ALM to determine the next mode at each event (the instance of crossing the switching boundary). Time-stepping methods [Awrejcewicz & Lamarque, 2003; Moreau, 1988; Stewart & Trinkle, 1996] are especially developed methods which do not require the determination (in contrast to event-driven methods) of the instances of crossing the switching boundary. In this case, the LCP, NCP or ALM methods are used to determine the mode of the system at each time step.

If the contact between two bodies is very small (the point contact) then sliding friction force opposes the sliding relative velocity and can be successfully modeled by the use of classical one-dimensional Coulomb friction law. In this case, the friction torque (drilling friction) and its influence on sliding friction force can be neglected (since the contact point cannot transmit a torque). But there are many cases of dynamical behavior of mechanical systems (billiard ball, Thompson top, wobblestone, electric polishing machine) which cannot be mathematically modeled (in order to obtain correct numerical simulation) or explained by the use of assumption of one-dimensional dry friction model.

Contensou [1962] noticed that relative normal angular velocity (spin) is important for the dynamics of some mechanical systems, where contact between two bodies or spin is relatively large. Based on the Coulomb friction law, he presented friction force as a function of two variables: relative sliding velocity of the center of the nonpoint circular contact area between two interacting bodies and relative normal angular velocity. He presented results in the integral and numerical forms for the contact stress distribution according to Hertz theory. Then the results of Contensou were essentially developed by Zhuravlev [1998, 2003] by giving exact analytical expressions for friction force and torque as well as corresponding linear Padé approximations that are more convenient to use in practical problems of modeling and simulation. We will refer to coupled model of friction force and torque as Coulomb–Contensou fritction model. This direction of research led to the second-order Padé

approximants [Zhuravlev & Kireenkov, 2005], more accurate and suitable for qualitative analysis. By the use of the same methodology, one can approach the problem of friction modeling in the case of axial symmetry of the contact stress distribution over the contact area [Kireenkov, 2005] (the elliptic contact patch with hertzian stress distribution is such a case). The integral forms of coefficients of the corresponding Padé approximants were given, however without any concrete, even numerical example. A three-dimensional friction model for circular areas but with the coupling between friction and rolling resistance, where rolling resistance is a result of distortion of contact stress distribution was developed in the work [Kireenkov, 2008]. Similar distortion of the normal stress distribution was used earlier in the modeling of the rolling resistance of the mobile tire [Svedenius, 2003]. One can notice that the proposed model of rolling resistance is compatible and logically coherent with the mechanism of rolling friction caused by elastic hysteresis losses (the main component of rolling resistance in many real systems) [Greenwood & Tabor, 1958; Greenwood *et al.*, 1961; Johnson, 1985; Tabor, 1955].

In the work [Leine & Glocker, 2003] the coupled friction model for circular contact area with central symmetry of contact stress distribution (without rolling resistance) was approximated by the use of Taylor expansion of the velocity pseudo potential and then used in the Thompson top modeling and simulation. The piecewise linear approximation of the three-dimensional friction model for elliptic contact area and the Hertz stress distribution (without rolling resistance) was presented in [Kosenko & Aleksandrov, 2009], where it was shown that the proposed model is more accurate than linear Padé approximants. Friedl [1997] in his work on the Thompson top modeling used the Tangens hyperbolicus approximation of the coupled integral friction model but only for the friction force component (the friction torque was neglected).

As mentioned above, there were some approaches to model rolling resistance along with the friction modeling. However here appears a question of the nature of rolling friction. Classically, it is understood as a resistance against a relative angular velocity of the contacting bodies tangential to the tangent plane of contact. But this model leads often to cumbersome and questionable results. Some authors introduced the concept of contour friction as resistance against the movement of contact point along the body [Leine, 2009; Leine *et al.*, 2005; Leine & van de Wouw, 2008]. These two models give the same results in some special cases (for example, when there is no slip between contacting bodies), but in general, are essentially different. However the proposed models of contour friction do not take into account the shape of the contact patch. Moreover, the coupling with the contact stress distribution and components of the dry friction model is also neglected.

One of the dynamical systems when the spatial Coulomb–Contensou friction as well as the rolling resistance is essential in dynamical behavior is the Celtic stone also known as wobblestone or rattleback. It is usually a semi-ellipsoidal solid (or another kind of body with smoothly curved oblong lower surface) with the special mass distribution. Most celts lie on a flat horizontal surface and are set in rotational motion about the vertical axis rotating in only one direction. The imposition of an initial spin in the opposite direction leads to transverse wobbling and then to spinning in the "preferred" direction. The Celtic stone with its special dynamical properties was an object of investigation of many researchers and the first scientific publication on this subject appeared towards the end of the 19th century [Walker, 1896].

One of the widely used assumptions in modeling of the celt is that of dissipation-free rolling without slip [Walker, 1896; Bondi, 1986; Lindberg & Longman, 1983; Borisov & Mamaev, 2003; Borisov *et al.*, 2006]. In the work of Walker [1986] the noncoincidence of the principal axes of inertia and the principal directions of curvature at the equilibrium contact point were pointed out as essential in the explanation of the wobblestone properties. Borisov and Mamaev [2003], and Borisov *et al.* [2006] presented transitions between regular and chaotic dynamics by the use of three-dimensional Poincaré maps and investigated stability of permanent vertical rotations of the nonholonomic dynamical system of the Celtic stone.

In work of Magnus [1974] an attempt of analysis of the linearized equations of the model assuming continuous slipping (quasi-viscous relation between the friction force and the velocity of the contact point) was performed. Another model taking into account dissipation but being far from reality is analyzed by the use of asymptotic perturbation theory [Caughey, 1980]. The model assuming rolling without slip and viscous damping (torque about all three axes) was proposed by Kane and Levinson [1982]. More realistic modeling with aerodynamic

dissipation and slip with dry friction force, with the addition of experimental validation of the model were presented by Garcia and Hubbard [1988]. In the work by Markeev [2002] the perturbation analysis of local dynamics around the equilibrium points of the model assuming the absence of friction as well as the experimental verification was performed. The closest to reality modeling of the celt was proposed by Zhuravlev and Klimov [2008], where the possibility of the slip was assumed, but in contrast to all the earlier works, the spatial Coulomb–Contensou friction model with linear Padé approximations for circular contact patch [Zhuravlev, 1998] was applied. However, since the friction force was the only way of dissipation in the proposed model, the time of the wobblestone motion (until rest) was unrealistically long.

In the present work, we propose for the first time the complete set of Tangens hyperbolicus approximations of the coupled model of dry friction and rolling resistance for circular contact area and compare them to the corresponding Padé approximants. Then the developed model is applied to the analysis of Celtic stone dynamics. The paper is organized as follows. In Sec. 2 the integral model of friction force and torque for circular shape of contact with hertzian normal stress distribution with special distortion modeling a coupling between dry friction and rolling resistance is introduced. Then the corresponding approximations of the integral model are presented. In Sec. 3, the mathematical model of the wobblestone as well as the implementation of the approximated models of dry friction and rolling resistance are given. Section 4 is devoted to some numerical examples comparing the response of the rattleback for different approximations of the integral friction model. The analysis of the response dependence on initial conditions is also performed by the use of a special kind of diagram. Section 5 gives some final remarks.

2. Model of Friction and Its Approximations

In Fig. 1, is presented a nondimensional circular contact area (of radius equal to one) with the center at point A, with relative translational nondimensional velocity of length $u = v_A/\rho$ (where v_A is the length of real sliding velocity of point A and ρ is the real radius of contact surface) and relative angular velocity ω. Without loss of generality, we assume that the velocity u is directed along the

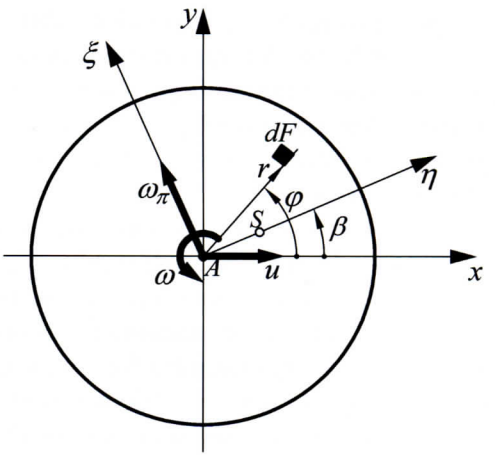

Fig. 1. The contact patch and co-ordinate systems.

x axis of the introduced co-ordinate system Axy. We assume that in the contact pressure distribution initially possessing central symmetry appears distortion due to the rolling resistance and the final stress distribution is symmetric with respect to the η axis of the $A\eta\xi$ co-ordinate system. The resultant normal force is applied at the point S and the rolling resistance vector is opposite to the ξ axis.

The resultant nondimensional friction force components and friction torque can be expressed as follows

$$\begin{aligned} T_x(u,\omega,\beta) &= T_{0x} + T_{rx}, \\ T_y(u,\omega,\beta) &= T_{0y} + T_{ry}, \\ M(u,\omega,\beta) &= M_0 + M_r, \end{aligned} \tag{1}$$

where T_{0x}, T_{0y} and M_0 are the corresponding friction force components along x and y axes and friction torque in the absence of rolling resistance while T_{rx}, T_{ry} and M_r are the corresponding components of friction force and torque related to rolling resistance. Assuming that Coulomb's law holds on an arbitrary surface element dF, the corresponding nondimensional elements of friction model (with nondimensional friction coefficient equal to one) have the following integral form in the polar co-ordinate system

$$T_{0x}(u,\omega) = \int_0^{2\pi}\int_0^1 \sigma_0 t_x \, dr d\varphi,$$

$$T_{rx}(u,\omega,\beta) = \int_0^{2\pi}\int_0^1 \sigma_r t_x \, dr d\varphi,$$

$$T_{0y}(u,\omega) = \int_0^{2\pi}\int_0^1 \sigma_0 t_y \, dr d\varphi,$$

$$T_{ry}(u,\omega,\beta) = \int_0^{2\pi}\int_0^1 \sigma_r t_y dr d\varphi,$$

$$M_0(u,\omega) = r\int_0^{2\pi}\int_0^1 \sigma_0(t_y\cos\varphi - t_x\sin\varphi)drd\varphi,$$

$$M_r(u,\omega,\beta) = r\int_0^{2\pi}\int_0^1 \sigma_r(t_y\cos\varphi - t_x\sin\varphi)drd\varphi, \tag{2}$$

where

$$t_x(r,\varphi) = \frac{r(u-\omega r\sin\varphi)}{\sqrt{u^2 - 2\omega ur\sin\varphi + \omega^2 r^2}},$$

$$t_y(r,\varphi) = \frac{\omega r^2\cos\varphi}{\sqrt{u^2 - 2\omega ur\sin\varphi + \omega^2 r^2}},$$

while σ_0 and σ_r are components of the nondimensional contact stress distribution $\sigma(r,\varphi,\beta) = \sigma_0(r) + \sigma_r(r,\varphi,\beta)$. It should be noted that σ_0 has central symmetry $T_{0y} = 0$.

The distortion in stress distribution related to the rolling resistance is assumed to be linear function with one parameter $0 \le k_r \le 1$ [Kireenkov, 2008]

$$\sigma_r(r,\varphi,\beta) = \sigma_0(r)k_r r\cos(\varphi-\beta), \tag{3}$$

where σ_0 is nondimensional (for the nondimensional surface element dF and additionally related to the real resultant normal reaction) contact stress distribution for the case without rolling resistance, which for the Hertz law takes the form

$$\sigma_0(r) = \frac{3}{2\pi}\sqrt{1-r^2}. \tag{4}$$

The integral models (1) and (2) is not convenient in direct application to real problems of modeling and simulation. Moving the origin of the polar co-ordinate system to the instantaneous center of velocities, one can obtain exact analytical expressions of the components (2) in elementary functions [Kireenkov, 2008]. But they are still inconvenient to use because of their complexity. A way to avoid this problem is to construct suitable approximations.

One of the simplest approximations is the first-order Padé proposed by Kireenkov [2008] for the complete combined model of sliding and rolling resistance in the following form

$$T_{0x(\mathrm{P1})} = \frac{u}{u + a_{11}|\omega|},$$

$$T_{rx(\mathrm{P1})} = a_{21}\frac{\omega k_r\sin\beta}{u + a_{11}|\omega|},$$

$$T_{ry(\mathrm{P1})} = b_{01}\frac{\omega k_r\cos\beta}{|\omega| + b_{11}u},$$

$$M_{0(\mathrm{P1})} = c_{01}\frac{\omega}{|\omega| + c_{11}u},$$

$$M_{r(\mathrm{P1})} = c_{21}\frac{uk_r\sin\beta}{|\omega| + c_{11}u}. \tag{5}$$

The coefficients of the model (5) are determined by the following conditions

$$\left.\frac{\partial T_{0x(\mathrm{P1})}}{\partial u}\right|_{u=0} = \left.\frac{\partial T_{0x}}{\partial u}\right|_{u=0}, \quad T_{rx(\mathrm{P1})}|_{u=0} = T_{rx}|_{u=0},$$

$$T_{ry(\mathrm{P1})}|_{u=0} = T_{ry}|_{u=0}, \quad \left.\frac{\partial T_{ry(\mathrm{P1})}}{\partial\omega}\right|_{\omega=0} = \left.\frac{\partial T_{ry}}{\partial\omega}\right|_{\omega=0},$$

$$M_{0(\mathrm{P1})}|_{u=0} = M_0|_{u=0}, \quad \left.\frac{\partial M_{0(\mathrm{P1})}}{\partial\omega}\right|_{\omega=0} = \left.\frac{\partial M_0}{\partial\omega}\right|_{\omega=0},$$

$$M_{r(\mathrm{P1})}|_{\omega=0} = M_r|_{\omega=0},$$

and for the Hertz case (4) we have $a_{11} = 8/(3\pi)$, $a_{21} = -1/4, b_{01} = 3\pi/32, b_{11} = 15\pi/32$, $c_{01} = 3\pi/16, c_{11} = 15\pi/16$, $c_{21} = -3\pi/16$. The approximations (5) preserve the values but do not completely satisfy all first partial derivatives of the functions (2) at $u = 0$ or $\omega = 0$.

To satisfy all first partial derivatives, it is necessary to use second-order Padé approximation [Kireenkov, 2008]

$$T_{0x(\mathrm{P2})} = \frac{u^2 + a_{12}u|\omega|}{u^2 + a_{12}u|\omega| + \omega^2},$$

$$T_{rx(\mathrm{P2})} = a_{22}\frac{|\omega|}{u^2+\omega^2}\omega k_r\sin\beta,$$

$$T_{ry(\mathrm{P2})} = b_{02}\frac{|\omega| + b_{12}u}{u^2 + b_{12}u|\omega| + \omega^2}\omega k_r\cos\beta, \tag{6}$$

$$M_{0(\mathrm{P2})} = c_{02}\frac{|\omega| + c_{12}u}{u^2 + c_{12}u|\omega| + \omega^2}\omega,$$

$$M_{r(\mathrm{P2})} = c_{22}\frac{u^2}{u^2+\omega^2}k_r\sin\beta.$$

Coefficients of the model (6) are determined analogically to the model (5) constants. For the Hertz case (4) we have $a_{12} = 8\pi/8, a_{22} = -3\pi/32$,

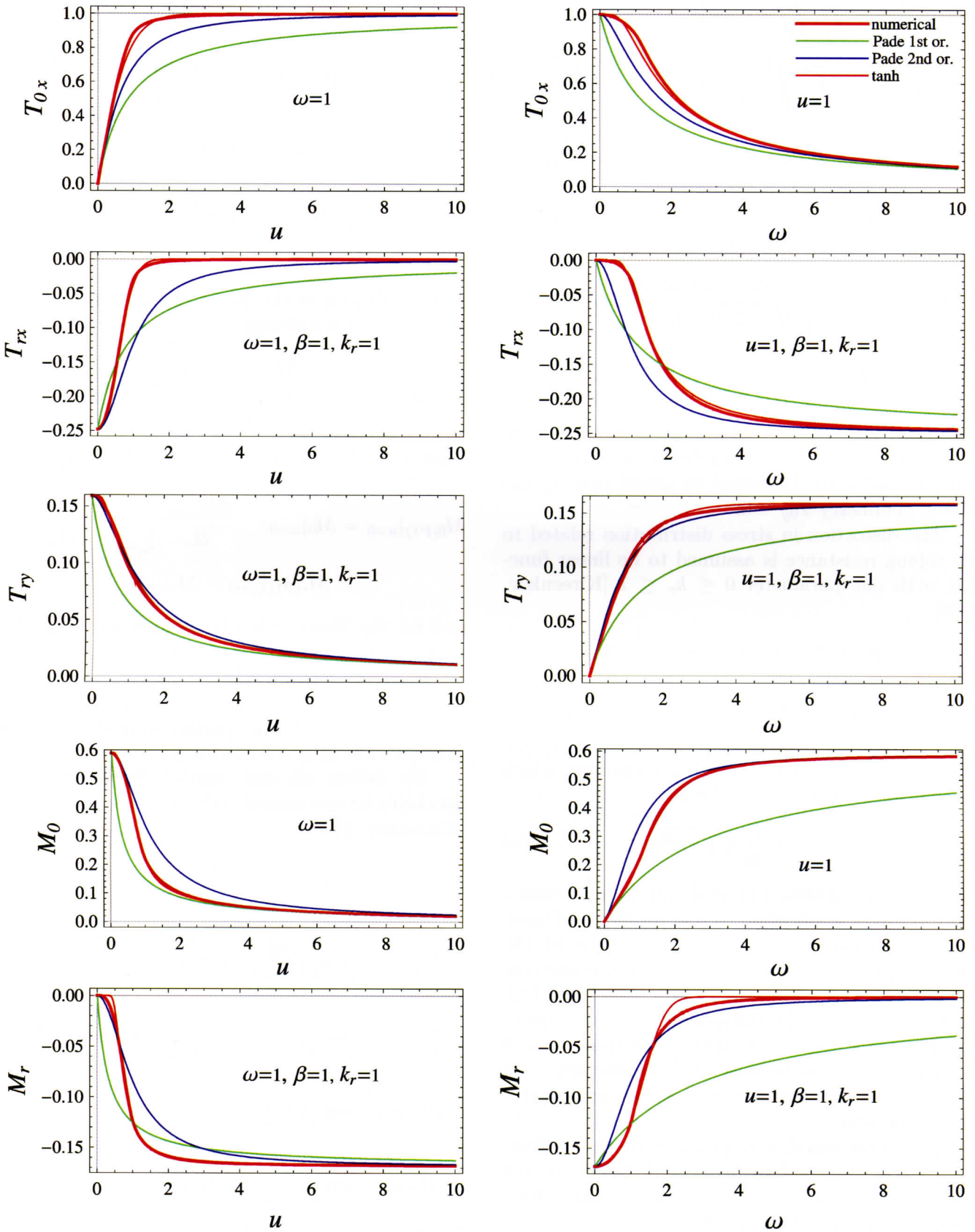

Fig. 2. Exact and approximated components of the friction models.

$b_{02} = 3\pi/32, b_{12} = 32/(15\pi), c_{02} = 3\pi/16, c_{12} = 16/(15\pi), c_{22} = -1/5$. The approximations (6) completely satisfy the values and all first partial derivatives of the functions (2) at $u = 0$ or $\omega = 0$.

In this paper for the first time, the complete set of Tangens hyperbolicus approximations of the coupled model of dry friction and rolling resistance for circular contact area between interacting bodies is proposed (similar approximation was used by Friedl [1997] in the Thompson top modeling, but only for T_{0x} component — the case with rolling resistance and friction torque is neglected) in the following form

$$\begin{aligned} T_{0x(\mathrm{th})} &= \tanh(h_1 u|\omega|^{-1}), \\ T_{rx(\mathrm{th})} &= f_1 k_r \sin\beta, \\ T_{ry(\mathrm{th})} &= f_2 k_r \cos\beta, \\ M_{0(\mathrm{th})} &= f_2 - f_1, \\ M_{r(\mathrm{th})} &= h_5(1 - \tanh(s_2 u^{-q_2}|\omega|^{q_2}))k_r \sin\beta, \end{aligned} \tag{7}$$

where

$$\begin{aligned} f_1 &= h_2(1 - \tanh(s_1 u^{q_1}|\omega|^{-q_1}))\,\mathrm{sign}(\omega), \\ f_2 &= h_3 \tanh(h_4 u^{-1}\omega). \end{aligned}$$

The coefficients of the model (7) are determined analogically to the models (5) and (6) case. The number of constants is smaller because of the use of certain relation between functions T_{rx}, T_{ry} and M_0 (the same relation can also be used for models (5) and (6), but we present them in the form proposed by Kireenkov [2008]). For the Hertz case (4) we have $h_1 = 3\pi/8, h_2 = -3\pi/32, h_3 = 3\pi/32$, $h_4 = 32/(15\pi)$, $h_5 = -1/5$. The approximations (7) completely satisfy the values and all first partial derivatives of the functions (2) at $u = 0$ or $\omega = 0$. Coefficients q_1, q_2, s_1, s_2 do not influence values and first partial derivatives at $u = 0$ or $\omega = 0$ but they are chosen to be $q_1 = 1.75$, $q_2 = 2.5, s_1 = 1.25, s_2 = 0.275$ for the best fitting of the integral model (2) for different values of u and ω.

Figure 2 presents the comparison of three approximated models (5)–(7) and exact integral model (2). It can be noted that the Tangens hyperbolicus approximation is closest to exact integral model. It is significantly more accurate than the second-order Padé approximation.

3. Celt Modeling

The wobblestone as a semi-ellipsoid rigid body with the mass center at the point C, touching a rigid, flat and immovable horizontal surface π (parallel to the XY plane of the global immovable co-ordinate system $X_1X_2X_3$) at point A is presented in Fig. 3.

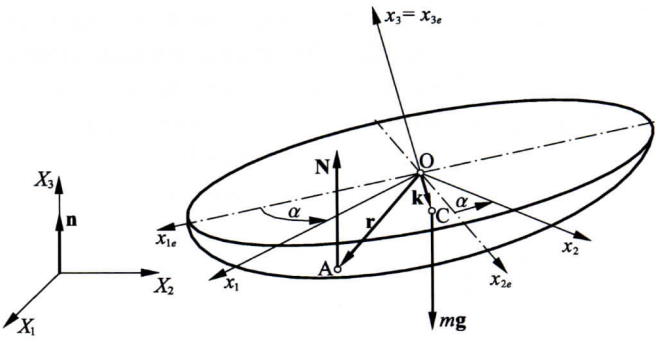

Fig. 3. The wobblestone on a horizontal plane π.

The equations of motion in the movable co-ordinate system $0x_1x_2x_3$ (with axes parallel to the central principal axes of inertia — we assume that geometrical axis x_{3e} of the ellipsoid is parallel to one of them) are as follows

$$\begin{aligned} m\frac{d\mathbf{v}}{dt} + \boldsymbol{\omega} \times (m\mathbf{v}) &= -mg\mathbf{n} + N\mathbf{n} + \mathbf{T}, \\ \mathbf{B}\frac{d\boldsymbol{\omega}}{dt} + \boldsymbol{\omega} \times (\mathbf{B}\mathbf{v}) &= (\mathbf{r} - \mathbf{k}) \times (N\mathbf{n} + \mathbf{T}) \\ &\quad + \mathbf{M}_t + \mathbf{M}_r, \\ \frac{d\mathbf{n}}{dt} + \boldsymbol{\omega} \times \mathbf{n} &= 0, \end{aligned} \tag{8}$$

where m is the mass of the celt, $\mathbf{B} = \mathrm{diag}(B_1, B_2, B_3)$ is the tensor of inertia of the solid, $\mathbf{v}$ is the absolute velocity of the mass center C, $\boldsymbol{\omega}$ is the absolute angular velocity of the body, N is the value of the normal reaction of the horizontal plane, $\mathbf{n}$ is the unit vector normal to the plane XY, $\mathbf{T}$ (ignored in Fig. 3) is the sliding friction force at the points of contact A, $\mathbf{M}_t$ and $\mathbf{M}_r$ (ignored in Fig. 3) are the dry friction and the rolling resistance torques applied to the body, respectively. Vector $\mathbf{r}$ indicates the actual contact point position and the vector $\mathbf{k}$ determines the mass center position.

The combined models of sliding friction and rolling resistance cannot be directly used in the form presented in Sec. 2 for celt modeling and simulations with the use of standard numerical methods of integration. One reason is that the expressions for friction forces and torques have singularity for $u = 0$ and $\omega = 0$. Another problem arises from the fact that for $u = 0$, the directions of the components T_{rx} and T_{ry} are indefinite. For that reason,

we will express them in the $A\eta\xi$ coordinate system. But the angle β will still be indefinite for lack of sliding velocity. Similar problems appear in the absence of rolling. In order to avoid the mentioned problems, we propose the following specific approximations and regularizations of the friction and rolling resistance models

$$\begin{aligned}\mathbf{T} &= -\mu N \mathbf{T}_{0(a)} \\ &\quad - \mu N (T_{rx(a)} c_\beta + T_{ry(a)} s_\beta) \frac{\boldsymbol{\omega}_\beta}{\|\boldsymbol{\omega}_\beta\| + \varepsilon} \\ &\quad - \mu N (T_{rx(a)} s_\beta - T_{ry(a)} c_\beta) \frac{\boldsymbol{\omega}_\pi}{\|\boldsymbol{\omega}_\pi\| + \varepsilon}, \\ \mathbf{M}_t &= -\mu \rho N M_{t(a)} \mathbf{n}, \quad \mathbf{M}_r = -\frac{f_r N \boldsymbol{\omega}_\pi}{\|\boldsymbol{\omega}_\pi\| + \varepsilon},\end{aligned} \tag{9}$$

where (a) in the end of index stands for some kind of approximation.

For linear Padé approximation, we have

$$\begin{aligned}\mathbf{T}_{0(\mathrm{P1}\varepsilon)} &= \frac{\mathbf{u}}{\|\mathbf{u}\| + a_{11}|\omega_n| + \varepsilon}, \\ T_{rx(\mathrm{P1}\varepsilon)} &= a_{21} \frac{\omega_n k_r s_\beta}{\|\mathbf{u}\| + a_{11}|\omega_n| + \varepsilon}, \\ T_{ry(\mathrm{P1}\varepsilon)} &= b_{01} \frac{\omega_n k_r c_\beta}{|\omega_n| + b_{11}\|\mathbf{u}\| + \varepsilon}, \\ M_{t(\mathrm{P1}\varepsilon)} &= \frac{c_{01}\omega_n + c_{21}\|\mathbf{u}\| k_r s_\beta}{|\omega_n| + c_{11}\|\mathbf{u}\| + \varepsilon}\end{aligned} \tag{10}$$

and the second-order Padé approximation model takes the form

$$\begin{aligned}\mathbf{T}_{0(\mathrm{P2}\varepsilon)} &= \frac{\|\mathbf{u}\| + a_{12}|\omega_n|}{\mathbf{u}^2 + a_{12}\|\mathbf{u}\||\omega_n| + \omega_n^2 + \varepsilon}\mathbf{u}, \\ T_{rx(\mathrm{P2}\varepsilon)} &= a_{22} \frac{|\omega_n|\omega_n k_r s_\beta}{\mathbf{u}^2 + \omega_n^2 + \varepsilon}, \\ T_{ry(\mathrm{P2}\varepsilon)} &= b_{02} \frac{|\omega_n| + b_{12}\|\mathbf{u}\|}{\mathbf{u}^2 + b_{12}\|\mathbf{u}\||\omega_n| + \omega_n^2 + \varepsilon}\omega_n k_r c_\beta, \\ M_{t(\mathrm{P2}\varepsilon)} &= \frac{|\omega_n| + c_{12}\|\mathbf{u}\|}{\mathbf{u}^2 + c_{12}\|\mathbf{u}\||\omega_n| + \omega_n^2 + \varepsilon}\omega_n \\ &\quad + c_{22} \frac{\mathbf{u}^2 k_r s_\beta}{\mathbf{u}^2 + \omega_n^2 + \varepsilon},\end{aligned} \tag{11}$$

while the Tangens hyperbolicus model will be as follows

$$\begin{aligned}\mathbf{T}_{0(\mathrm{th}\varepsilon)} &= \tanh\left(h_1 \frac{\|\mathbf{u}\|}{|\omega_n| + \varepsilon}\right) \frac{\mathbf{u}}{\|\mathbf{u}\| + \varepsilon}, \\ T_{rx(\mathrm{th}\varepsilon)} &= f_{1\varepsilon} k_r s_\beta, \\ T_{ry(\mathrm{th}\varepsilon)} &= f_{2\varepsilon} k_r c_\beta, \\ M_{t(\mathrm{th}\varepsilon)} &= f_{2\varepsilon} - f_{1\varepsilon} \\ &\quad + h_5\left(1 - \tanh\left(s_2\left(\frac{|\omega_n| + \varepsilon}{\|\mathbf{u}\|}\right)^{q_2}\right)\right) k_r s_\beta,\end{aligned} \tag{12}$$

where

$$\begin{aligned}f_{1\varepsilon} &= h_2\left(1 - \tanh\left(s_1\left(\frac{\|\mathbf{u}\|}{|\omega_n| + \varepsilon}\right)^{q_1}\right)\right)\operatorname{sign}(\omega_n) \\ \text{and} \quad f_{2\varepsilon} &= h_3 \tanh\left(h_4 \frac{\omega_n}{\|\mathbf{u}\| + \varepsilon}\right),\end{aligned}$$

where μ is the dry friction coefficient, ρ is the radius of the contact patch (we assume circular contact patch between bodies with constant radius independent from normal force), $f_r = \rho \int_0^{2\pi} \int_0^1 \sigma_r r^2 \cos(\varphi - \sigma) dr d\varphi$ is the rolling resistance coefficient and for the Hertz case $f_r = \rho k_r / 5$, $\mathbf{u}$ is the normalized velocity $\mathbf{v}_A$ of the body point when in contact with the horizontal surface, ω_n is the projection of angular velocity on the X_3 axis, $\boldsymbol{\omega}_\pi$ is the component of angular velocity lying in the π plane, $\boldsymbol{\omega}_\beta$ is the vector lying in the π plane of the same length as $\boldsymbol{\omega}_\pi$ but perpendicular to $\boldsymbol{\omega}_\pi$, c_β and s_β are approximated sine and cosine functions of the angle β (angle between the sliding and rolling directions):

$$\begin{aligned}\mathbf{v}_A &= \mathbf{v} + \boldsymbol{\omega} \times (\mathbf{r} - \mathbf{k}), \quad \mathbf{u} = \frac{\mathbf{v}_A}{\rho}, \\ \omega_n &= \boldsymbol{\omega} \cdot \mathbf{n}, \quad \boldsymbol{\omega}_\pi = \boldsymbol{\omega} - \omega_n \mathbf{n}, \quad \boldsymbol{\omega}_\beta = \boldsymbol{\omega}_\pi \times \mathbf{n}, \\ c_\beta &= \frac{u_\eta}{\|\mathbf{u}\| + \varepsilon_1}, \quad s_\beta = \operatorname{sgn}_1(u_\xi)\sqrt{1 - c_\beta^2}, \\ u_\eta &= \mathbf{u} \cdot \boldsymbol{\omega}_\beta, \quad u_\xi = -\mathbf{u} \cdot \boldsymbol{\omega}_\pi, \\ \operatorname{sgn}_1(u_\xi) &= \begin{cases} 1 & \text{for } u_\xi \geq 0 \\ -1 & \text{for } u_\xi < 0. \end{cases}\end{aligned} \tag{13}$$

The $\mathbf{M}_r$ vector is constructed with assumption that the rolling resistance torque opposes the angular velocity component lying in the π plane (it is equivalent to assumption of rigid π plane and deformable wobblestone). The parameters ε and ε_1 are introduced in order to smooth the

equations and avoid numerical problems around some singularities.

The differential equations of motion (1) are supplemented by the following algebraic equation

$$(\mathbf{v} + \boldsymbol{\omega} \times (\mathbf{r} - \mathbf{k})) \cdot \mathbf{n} = 0, \tag{14}$$

which follows the fact that the velocity $\mathbf{v}_A$ lies in the plane π. Equations (8) and (14) form now the differential-algebraic equation set. One way to solve them is to differentiate the condition (14) with respect to time

$$\left[\frac{d\mathbf{v}}{dt} + \frac{d\boldsymbol{\omega}}{dt} \times (\mathbf{r} - \mathbf{k}) + \boldsymbol{\omega} \times \frac{d\mathbf{r}}{dt} + \boldsymbol{\omega} \times (\mathbf{v} + \boldsymbol{\omega} \times (\mathbf{r} - \mathbf{k}))\right] \cdot \mathbf{n} = 0, \tag{15}$$

and then treat it as an additional equation when solving the governing equations algebraically with respect to the corresponding derivatives and the normal reaction N.

To complete the model the relation between the vectors $\mathbf{r}$ and $\mathbf{n}$ should be given. Taking the ellipsoid equation

$$\phi(\mathbf{r}) = \frac{r_{1e}^2}{a^2} + \frac{r_{2e}^2}{b^2} + \frac{r_{3e}^2}{c^2} - 1 = 0, \tag{16}$$

(where a, b and c are the semi-axes of the ellipsoid along the axes x_{1e}, x_{2e} and x_{3e} respectively) and the condition of tangent contact between the ellipsoid and the horizontal plane

$$\mathbf{n} = \mu \frac{d\phi}{d\mathbf{r}}, \tag{17}$$

where $\mu < 0$ is a certain scalar multiplier, we can find the following relation between the components of the vectors $\mathbf{r}$ and $\mathbf{n}$ in the $0x_{1e}x_{2e}x_{3e}$ coordinate system

$$r_{1e} = \frac{a^2 n_{1e}}{2\mu}, \quad r_{2e} = \frac{b^2 n_{2e}}{2\mu}, \quad r_{3e} = \frac{c^2 n_{3e}}{2\mu}, \tag{18}$$

where

$$\mu = -\frac{1}{2}\sqrt{a^2 n_{1e}^2 + b^2 n_{2e}^2 + c^2 n_{3e}^2}. \tag{19}$$

Because we use the differentiated form (15) of the algebraic condition (14), the differentiated relations (18) will be needed

$$\begin{aligned}
\dot{r}_{1e} &= \frac{a^2[\dot{n}_{1e}(b^2 n_{2e}^2 + c^2 n_{3e}^2) - n_{1e}(b^2 n_{2e}\dot{n}_{2e} + c^2 n_{3e}\dot{n}_{3e})]}{8\mu^3}, \\
\dot{r}_{2e} &= \frac{b^2[\dot{n}_{2e}(a^2 n_{1e}^2 + c^2 n_{3e}^2) - n_{2e}(a^2 n_{1e}\dot{n}_{1e} + c^2 n_{3e}\dot{n}_{3e})]}{8\mu^3}, \\
\dot{r}_{3e} &= \frac{c^2[\dot{n}_{2e}(a^2 n_{1e}^2 + b^2 n_{2e}^2) - n_{3e}(a^2 n_{1e}\dot{n}_{1e} + b^2 n_{2e}\dot{n}_{2e})]}{8\mu^3}.
\end{aligned} \tag{20}$$

Since the $0x_1x_2x_3$ co-ordinate system is obtained by rotation of the $0x_{1e}x_{2e}x_{3e}$ system around the x_{3e} axis by the angle α, the corresponding relation in the $0x_1x_2x_3$ co-ordinate system can be found easily.

4. Numerical Simulations

All the results presented in the paper have been obtained for the following parameters and initial conditions: $m = 0.25\,\mathrm{kg}$, $g = 10\,\mathrm{m/s^2}$, $\alpha = -0.3\,\mathrm{rad}$, $B_1 = 10^{-4}\,\mathrm{kg \cdot m^2}$, $B_2 = 8 \cdot 10^{-4}\,\mathrm{kg \cdot m^2}$, $B_3 = 10^{-3}\,\mathrm{kg \cdot m^2}$, $a = 0.08\,\mathrm{m}$, $b = 0.016\,\mathrm{m}$, $c = 0.012\,\mathrm{m}$, $k_1 = k_2 = 0$, $k_3 = -0.002\,\mathrm{m}$, $\mu = 0.5, \rho = 6 \cdot 10^{-4}\,\mathrm{m}$, $k_r = 1$, $\varepsilon = 10^{-4}\,\mathrm{rad/s}$, $\varepsilon_1 = 10^{-12}\,\mathrm{rad/s}$, $v_{10} = v_{20} = v_{30} = 0\,\mathrm{m/s}$, $n_{10} = n_{20} = 0$, $n_{30} = 1$.

Figure 4 show the results of simulation of the celt initially spinning with $\omega_{30} = 20\,\mathrm{rad/s}$ but also wobbling with $\omega_{20} = 1\,\mathrm{rad/s}$ ($\omega_{10} = 0$) for three different approximations: the first-order Padé, the second-order Padé and Tangens hyperbolicus approximations. The celt exhibits typical kind of solid behavior, that is, we can observe after some time the spin changes sign and then the motion vanishes. The differences between three solutions are seen, especially between the solution with the use of the first-order Padé approximation and the others. To answer the question of significance of that difference depends on the kind of application of the developed model and simulation. The rest of the presented results have been obtained by using Tangens hyperbolicus approximation.

Figure 5 presents similar results for the initial spin $\omega_{30} = 4\,\mathrm{rad/s}$ and wobbling with $\omega_{20} = 1\,\mathrm{rad/s}$ ($\omega_{10} = 0$). We can also see the corresponding behavior of the system with friction torque M_t switched off, where the motion ends with the celt spinning

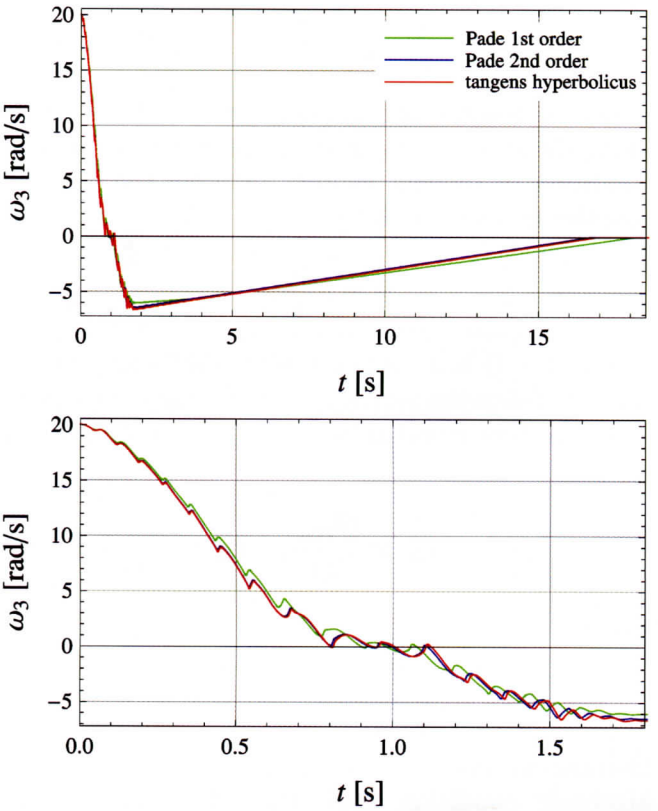

Fig. 4. The wobblestone response with initial conditions $\omega_{10} = 0$, $\omega_{20} = 1, \omega_{30} = 20\,(\mathrm{rad/s})$ for different approximations of the friction model.

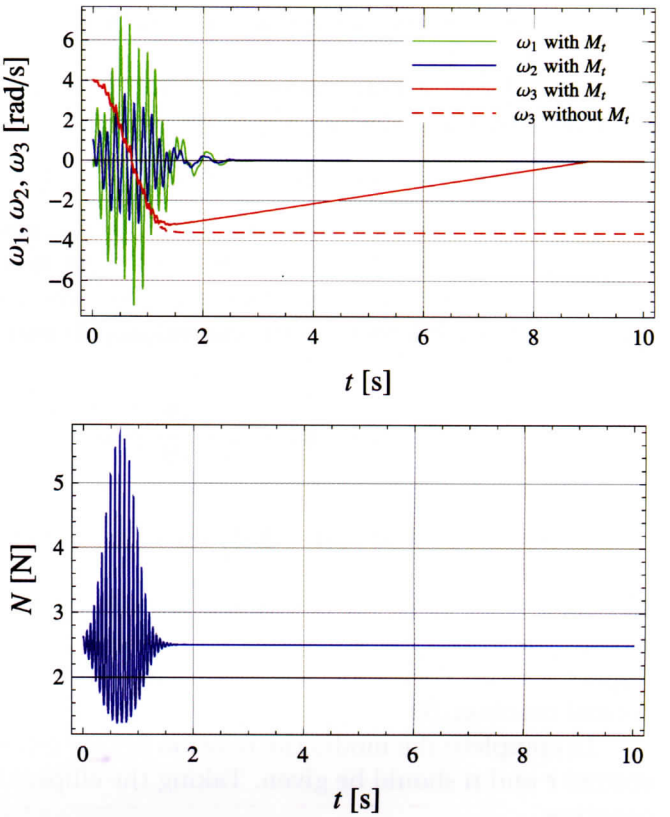

Fig. 5. The wobblestone response and normal force history with initial conditions $\omega_{10} = 0, \omega_{20} = 1, \omega_{30} = 4\,(\mathrm{rad/s})$ for Tangens hyperobolicus approximation.

with constant velocity without wobbling, but the initial portion of motion do not differ significantly from the motion of the celt with the friction torque. The corresponding normal force history is also presented in Fig. 5.

In Fig. 6 the final ω_3 angular velocity for the celt without dry friction torque M_t for different initial conditions is presented in the form of contour plots. One observes that for one direction of the spin [$\omega_{30} = 2\,\mathrm{rad/s}$ in Fig. 6(a)] there is some area around the point $(0, 0)$ on the plane of initial conditions ω_{10}–ω_{20} for which there are no reversals. The change of sign of spin takes place for initial conditions outside that area, that is, for the initial wobbling strong enough. For the opposite sign of the initial spin [$\omega_{30} = -3\,\mathrm{rad/s}$ in Fig. 6(b)] it is difficult to observe the spin reversal. It is most interesting to see the plot from Fig. 6(c), where the section along the ω_{30} axis in the initial conditions space is shown. It is seen that the ω_3 axis is stable in that sense, the perturbation of the wobblestone spinning with any value is small enough and any sign will decay after a while, and the stone will continue spinning with (almost) the same velocity. To observe the reversals, the initial wobbling must be large enough and only for the proper sign of the spin.

5. Concluding Remarks

For the first time the complete set of Tangens hyperbolicus approximations of the spatial friction model coupled with the rolling resistance for circular contact area between interacting bodies has been developed and then compared with the corresponding Padé approximants of the first- and second-order well known from the literature and with the numerical solution of the exact integral model as well. It has been shown that Tangens hyperbolicus approximants are closest to the exact solution. Applying three different approximations to the celtic stone model the differences in simulation results have been shown. In applications when high accuracy of simulation is required, the model with second-order Padé or Tangens hyperbolicus approximations should be used. Taking into account that complexity of both approximations are comparable and that

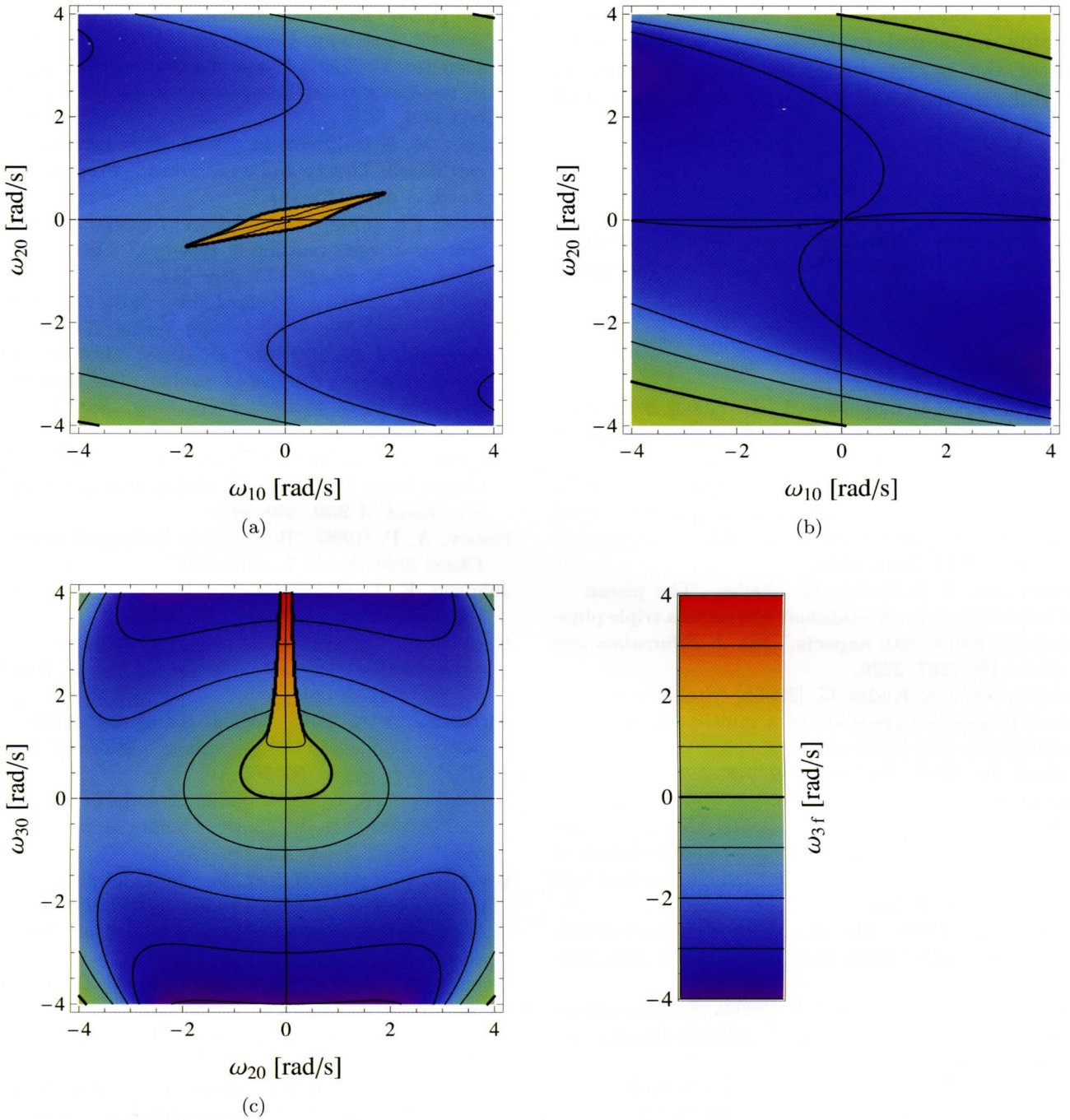

Fig. 6. The wobblestone final ω_3 angular velocity (rad/s) (without dry friction torque M_t) for different initial conditions: (a) $\omega_{30} = 2\,\mathrm{rad/s}$, (b) $\omega_{30} = -3\,\mathrm{rad/s}$, (c) $\omega_{10} = 0\,\mathrm{rad/s}$.

the Tangens hyperbolicus approximation is actually closer to the exact integral model of friction, it seems to be reasonable to use the second one.

Both presented model of the celt and its simulations are very realistic, when compared with most earlier works on the celt, since the correct spatial friction model coupled with the rolling resistance torque have been applied, however with the significant simplifying assumption of circular contact area between stone and the table with constant radius independent from the normal force. In the next step, we are going to extend the model of friction and its approximations to the elliptic contacts. The presented results of the celt simulations are selective and more systematic research of that object is required as well as careful experimental validation should be performed. The proposed smoothing of the governing equations should be

treated as temporary and a substitute method of avoiding numerical problems and certain extension of the model should be made in order to join different modes of dynamics (for example stick and slip).

Acknowledgment

The work has been supported by the Ministry of Science and Higher Education under the grant no. 0040/B/T02/2010/38.

References

Awrejcewicz, J. & Lamarque, C.-H. [2003] *Bifurcation and Chaos in Nonsmooth Mechanical Systems* (World Scientific, Singapore).

Awrejcewicz, J., Kudra, G. & Lamarque, C.-H. [2004] "Investigation of triple pendulum with impacts using fundamental solution matrices," *Int. J. Bifurcation and Chaos* **14**, 4191–4213.

Awrejcewicz, J. & Kudra, G. [2005a] "The piston — Connecting rod — Crankshaft system as a triple physical pendulum with impacts," *Int. J. Bifurcation and Chaos* **15**, 2207–2226.

Awrejcewicz, J. & Kudra, G. [2005b] "Stability analysis and Lyapunov exponents of a multi-body mechanical system with rigid unilateral constraints," *Nonlin. Anal. Th. Meth. Appl.* **63**, 909–918.

Awrejcewicz, J., Supeł, B., Lamarque, C.-H., Kudra, G., Wasilewski, G. & Olejnik, P. [2008] "Numerical and experimental study of regular and chaotic motion of triple physical pendulum," *Int. J. Bifurcation and Chaos* **18**, 2883–2915.

Bondi, Sir H. [1986] "The rigid body dynamics of unidirectional spin," *Proc. Roy. Soc. Lond. A* **405**, 265–279.

Borisov, A. V. & Mamaev, I. S. [2003] "Strange attractors in rattleback dynamics," *Physics-Uspekhi* **46**, 393–403.

Borisov, A. V., Kilin, A. A. & Mamaev, I. S. [2006] "New effects of rattlebacks," *Dokl. Phys.* **51**, 272–275.

Brogliato, B. [1999] *Nonsmooth Mechanics* (Springer-Verlag, London).

Caughey, T. K. [1980] "A mathematical model of the rattleback," *Int. J. Non-lin. Mech.* **15**, 293–302.

Contensou, P. [1962] "Couplage entre frottement de glissement et frottement de pivotement dans la téorie de la toupe," *Kreiselprobleme Gyrodynamics: IUTAM Symp.*, Calerina, pp. 201–216.

Fillipov, A. [1988] *Differential Equations with Discontinuous Right-Hand Sides* (Kluwer Academic Publishers, Dortrecht).

Friedl [1997] "Der Stehaufkreisel," Master's thesis, Universität Augsburg, Germany.

Galvanetto, U. [2001] "Some discontinuous bifurcations in two-block stick-slip system," *J. Sound Vibr.* **248**, 653–669.

Garcia, M. & Hubbard, M. [1988] "Spin reversal of the rattleback: Theory and experiment," *Proc. Roy. Soc. Lond. A* **418**, 165–197.

Glocker, Ch. [1999] "Formulation of spatial contact situations in rigid multibody systems," *Comput. Meth. Appl. Mech. Engin.* **177**, 199–214.

Glocker, Ch. [2001] *Set-Valued Force Laws, Dynamics of Non-Smooth Systems* (Springer-Verlag, Berlin).

Greenwood, J. A. & Tabor, D. [1958] "The friction of hard sliders on lubricated rubber: The importance of deformation losses," *Proc. Phys. Soc.* **71**, 989–1001.

Greenwood, J. A., Minshall, H. & Tabor, D. [1961] "Hysteresis losses in rolling and sliding friction," *Proc. R. Soc. Lond. A* **259**, 480–507.

Ivanov, A. P. [1996] "Bifurcations in impact systems," *Chaos Solit. Fract.* **7**, 1615–1634.

Johnson, K. L. [1985] *Contact Mechanics* (Cambridge University Press, Cambridge).

Kane, T. R. & Levinson, D. A. [1982] "Realistic mathematical modeling of a rattleback," *Int. J. Non-lin. Mech.* **17**, 175–186.

Kireenkov, A. A. [2005] "About the motion of the symmetric rigid solid along the plane," *8th Conf. DSTA*, Łódź, Poland, pp. 95–102.

Kireenkov, A. A. [2008] "Combined model of sliding and rolling friction in dynamics of bodies on a rough surface," *Mech. Solids* **43**, 116–131.

Kosenko, I. & Aleksandrov, E. [2009] "Implementation of the Contensou-Erisman model of friction in frame of the Hertz contact problem on Modelica," *7th Modelica Conf.*, Como, Italy, pp. 288–298.

Leine, R. I., Glocker, Ch. & van Campen, D. H. [2001] "Nonlinear dynamics of the woodpecker toy," *Proc. Design Engineering Technical Conf.*, Pittsburgh, CD-ROM, 8 pp.

Leine, R. I. & Glocker, Ch. [2003] "A set-valued force law for spatial Coulomb–Contensou friction," *European J. Mech. A/Solids* **22**, 193–216.

Leine, R. I. & Nijmeijer, H. [2004] *Dynamics and Bifurcations of Non-smooth Mechanical Systems* (Springer-Verlag, Berlin, NY).

Leine, R. I., Le Saux, C. & Glocker, Ch. [2005] "Friction models for the rolling disk," *Proc. 5th EUROMECH Nonlinear Dynamics Conference* (ENOC 2005), Eindhoven, The Netherlands.

Leine, R. I. & Van De Wouw, N. [2008] *Stability and Convergence of Mechanical Systems with Unilateral Constraints* (Springer-Verlag, Berlin, NY).

Leine, R. I. [2009] "Measurements of the finite-time singularity of the Euler disk," *7th EUROMECH Solid Mechanical Conf.*, Lisbon, Portugal.

Lindberg, R. E. & Longman, R. W. [1983] "On the dynamic behaviour of the wobblestone," *Acta Mechanica* **49**, 81–94.

Magnus, K. [1974] "Zur Theorie der keltischen Wackelsteine," *Zeitschrift für Angewandte Mathematik und Mechanik* **5**, 54–55.

Markeev, A. P. [2002] "On the dynamics of a solid on an absolutely rough plane," *Regul. Chaot. Dyn.* **7**, 153–160.

Moreau, J. J. [1988] "Unilateral contact and dry friction in finite freedom dynamics," *Non-smooth Mechanics and Applications*, eds. Moreau, J. J. & Panagiotopoulos, P. (Springer-Verlag, Wien), pp. 1–82.

Pfeiffer, F. & Glocker, Ch. [1996] *Multibody Dynamics with Unilateral Contacts* (Wiley, NY).

Pfeiffer, F. [2003] "The idea of complementarity in multibody dynamics," *Arch. Appl. Mech.* **72**, 807–816.

Shaw, S. W. & Holmes, P. [1983] "A periodically forced piecewise linear oscillator," *J. Sound Vibr.* **90**, 129–155.

Simpson, D. J. W. [2010] *Bifurcations in Piecewise-Smooth Continuous Systems* (World Scientific, Singapore).

Stewart, D. E. & Trinkle, J. C. [1996] "An implicit time-stepping scheme for rigid body dynamics with inelastic collisions and Coulomb friction," *Int. J. Numer. Meth. Engin.* **39**, 2673–2691.

Svedenius, J. [2003] *Tire Models for Use in Braking Application*, Licenciate thesis, Lund University.

Tabor, D. [1955] "The mechanism of rolling friction. II. The elastic range," *Proc. R. Soc. Lond. A* **229**, 198–220.

Virgin, L. N. & Begley, C. J. [1999] "Grazing bifurcations and basins of attraction in an impact-friction oscillator," *Physica D* **130**, 43–57.

Walker, G. T. [1896] "On a dynamical top," *Q. J. Pure App. Math.* **28**, 175–184.

Zhuravlev, V. Ph. [1998] "The model of dry friction in the problem of the rolling of rigid bodies," *J. Appl. Math. Mech.* **62**, 705–710.

Zhuravlev, V. P. [2003] "Friction laws in the case of combination of slip and spin," *Mech. Solids* **38**, 52–58.

Zhuravlev, V. Ph. & Kireenkov, A. A. [2005] "Padé expansions in the two-dimensional model of Coulomb friction," *Mech. Solids* **40**, 1–10.

Zhuravlev, V. P. & Klimov, D. M. [2005] "On the dynamics of the Thompson top (tippe top) on the plane with real dry friction," *Mech. Solids* **40**, 117–127.

Zhuravlev, V. Ph. & Klimov, D. M. [2008] "Global motion of the celt," *Mech. Solids* **43**, 320–327.